Wind and Structures, *Vol. 22, No. 3 (2016) 349-368*
DOI: http://dx.doi.org/10.12989/was.2016.22.3.349

Preconditioning technique for a simultaneous solution to wind-membrane interaction

Fang-jin Sun[1,2] and Ming Gu[*2]

[1]*College of Civil Engineering and Architecture, Liaoning Technical University, Fuxin, Liaoning,123000, China*
[2]*State Key Laboratory of Disaster Reduction in Civil Engineering, Tongji University, Shanghai 200092, China*

(Received June 11, 2015, Revised January 26, 2016, Accepted January 27, 2016)

Abstract. A preconditioning technique is presented for a simultaneous solution to wind-membrane interaction. In the simultaneous equations, a linear elastic model was employed to deal with the fluid-structure data transfer at the interface. A Lagrange multiplier was introduced to impose the specified boundary conditions at the interface and strongly coupled simultaneous equations are derived after space and time discretization. An initial linear elastic model preconditioner and modified one were derived by treating the linearized elastic model equation as a saddle point problem, respectively. Accordingly, initial and modified fluid-structure interaction (FSI) preconditioner for the simultaneous equations were derived based on the initial and modified linear elastic model preconditioners, respectively. Wind-membrane interaction analysis by the proposed preconditioners, for two and three dimensional membranous structures respectively, was performed. Comparison was made between the performance of initial and modified preconditioners by comparing parameters such as iteration numbers, relative residuals and convergence in FSI computation. The results show that the proposed preconditioning technique greatly improves calculation accuracy and efficiency. The priority of the modified FSI preconditioner is verified. The proposed preconditioning technique provides an efficient solution procedure and paves the way for practical application of simultaneous solution for wind-structure interaction computation.

Keywords: membrane structures; wind loading; fluid-structure interaction; simultaneous solution; preconditioning technique

1. Introduction

Fluid-structure interaction between wind and membrane structures is recognized as one of the most significant, yet not comprehensively studied, issues in the wind-resistant behaviour of flexible building structures. Numerical simulation has become a vigorous tool for fluid-structure interaction computation due to rapid progress in hardware and software of computers (Dagnew and Bitsuamlak 2013, 2014). Currently, numerical simulation methods fall into three categories, partitioned solutions with loosely-coupling method (Borna *et al*. 2013), partitioned solutions with strongly-coupling method and simultaneous solutions (Hermann and Jan 2002, 2003). In loosely-coupling partitioned solutions schemes, separate solvers for fluid and structure are

*Corresponding author, Professor, E-mail: minggu@tongji.edu.cn

http://www.techno-press.org/?journal=was&subpage=8 ISSN: 1226-6116 (Print), 1598-6225 (Online)

employed once per time step, resulting in a time lag between both continua, whereas strongly-coupling partitioned solutions require an additional iteration loop based on the partial solvers, which demonstrate better convergence and stability characteristics, but additional numerical efforts are needed. Simultaneous procedures solve the coupled system in a single iteration loop with consistent time integration schemes for all physical fields, resulting in time-accurate coupled solutions (Namkooong *et al*. 2005). In other words, an anthology of numerical simultaneous solution is applied to FSI of membrane structures under wind actions, including formulating the fluid-structure system in the form of simultaneous equations, and solving it simultaneously (Degroote *et al*. 2009, Habchi *et al*. 2013).

Most of the current studies on FSI of membrane structures, with numerical simulation, adopt partitioned solutions with loose-coupling or strong-coupling methods. Studies on simultaneous solution method have been rather limited (Habchi *et al*. 2013, Hachem *et al.* 2013). However, the limited study has shown its superiority in stability and accuracy in computation (Habchi *et al*. 2013, Michler *et al*. 2004) over partitioned solutions. Thus, for membrane structures undergoing large-displacement, a simultaneous solutions is preferable for wind-membrane structure interaction analysis since it ensures better stability and convergence.

One of the key aspects in fluid-structure interaction computation is data transfer at fluid-structure interface. Sun and Gu (2014) proposed a linear elastic model to deal with the fluid deformation to derive a single equation system for a simultaneous solution to compute wind-membrane interaction. For the simultaneous solution procedure, Newton's method is usually needed to linearize the simultaneous equations of the coupled system. In spite of its superiority in accuracy and stability of simultaneous solution method, large amounts of computational efforts are consumed on repeated integration of Jacobian matrix and Newton modification of the linearized simultaneous equations, which probably result in ill-conditioned of the linearized equations and inefficiency of simultaneous solution procedure. Thus, it is among the top priorities to solve the simultaneous equations effectively. Generalized minimum residual algorithm (GMRES for short), an iteration method, is one of Krylov subspace projections methods that commonly used to solve large asymmetric linear equations, exactly the case of linearized simultaneous equations (Manguoglu *et al.* 2011). A preconditioning technique, aggregating eigenvalues of linear iteration matrix to diminish computation time when solving linear equations, is usually required to accelerate convergence for the method.

For fluid-structure interaction, some preconditioning techniques have been proposed to solve the linearized nonlinear equations based on the current studies, which can fall into three categories. The first category is the preconditioning technique that modifies the boundary conditions at the fluid-structure interface, among which Dirichlet-Neumann boundary preconditioner is commonly used. The advantage of the method lies in its usage of existing CFD and CSD module and as a result, it is usually employed in partitioned solutions with loosely-coupling method (Heil *et al.* 2008). The second category is Schur preconditioner. Barker and Cai (2009, 2010) proposed preconditioner based on Newton-Krylov-Schwarz algorithm. In Barker and Cai (2009), Schwarz domain decomposition was adopted to solve strongly coupled equations. In Barker and Cai (2010), additional Schwarz preconditioner with double-layer computation method was proposed based on Krylov subspace solver. The third method is to employ blocked triangle preconditioner. Badia *et al*. (2008a, b) proposed incomplete LU decomposition (ILU for short) preconditioner and inaccurate blocked LU decomposition preconditioner to solve strongly coupled equations. In spite of the proposed preconditioners for strongly-coupled methods, they are only aimed at separate fluid solver or structural solver, that is, the preconditioners could be only used for fluid domain or

structural domain. Meanwhile, the preconditioners have not been validated for wind-membrane interaction computation due to large added-mass effect resulted from light weight of the membrane structures.

Linear elastic model was proposed to deal with the fluid domain deformation and strongly coupled simultaneous equations were derived by the authors of this paper (Sun and Gu 2014). The objective of this paper is to study preconditioning technique for the proposed strongly coupled simultaneous equations to solve the nonlinear equations efficiently and study wind-membrane interaction in a more accurate manner. A Lagrange multiplier is introduced to impose the boundary conditions on the fluid-structure interface. An initial linear elastic model preconditioner and modified one is derived by treating the linearized elastic model equation as a saddle point problem, respectively. The fluid-structure interaction (FSI) preconditioning matrix for the simultaneous equations is then derived based on the initial and modified linear elastic model preconditioning matrix. Wind-membrane interaction for two and three dimensional membrane structures using the proposed preconditioner were computed. The performance and efficiency of the preconditioners was evaluated.

2. Governing equations for fluid-structure interaction system

2.1 Governing equations

The incompressible viscous fluid is governed by the Navier–Stokes equations, consisting of momentum conservation and continuity equation. The governing equations for the structure are described by a total Lagrange (T.L.) formulation and a large deformation theory. A linear elastic model is introduced to deal with the data transfer at the interface, which is governed by semi-discretized finite element equations. These equations can be found in Sun and Gu (2014).

2.2 Coupling conditions

Each node i of the fluid, structure and linear elastic model is assumed to be connected with the fixed material point on the fluid-structure interface. The material point is denoted by its Lagrange coordinates ϑ^{i}, then the coupling conditions on the fluid-structure interface can be written as

$$\mathbf{u}_{ES}(\vartheta^1_{\Gamma I}(\lambda),\vartheta^2_{\Gamma I}(\lambda),\vartheta^3_{\Gamma I}(\lambda)) = \mathbf{u}_I(\lambda)\text{, on}\,\Gamma_I \tag{1}$$

$$\mathbf{v}_f^{FSI} = \mathbf{v}_s^{FSI}\text{,on}\,\Gamma_I \tag{2}$$

$$\boldsymbol{\sigma}_s^{FSI}(\mathbf{u}_I(\lambda))\cdot\mathbf{n}_s + \boldsymbol{\sigma}_f^{FSI}(\mathbf{u}_I(\lambda))\cdot\mathbf{n}_f = 0\text{, on}\,\Gamma_I \tag{3}$$

where $\mathbf{u}_{ES}$ denotes the displacement vector of the linear elastic model, $\mathbf{u}_I$ denotes the structure displacement on the interface Γ_I, λ denotes the peripheric coordinate form at the interface Γ_I, then, $(\vartheta^1,\vartheta^2,\vartheta^3)\big|_{\Gamma I} = (\vartheta^1_{\Gamma I}(\lambda),\vartheta^2_{\Gamma I}(\lambda),\vartheta^3_{\Gamma I}(\lambda))$. Eq. (1) indicates that the linear elastic model displacement equals the real structure displacement at the interface. Eq. (1) can be regarded as the Dirichlet condition imposed on the displacement field of the linear elastic model. $\mathbf{v}_f^{FSI}$ and $\mathbf{v}_s^{FSI}$

are fluid velocity and structure velocity at the interface Γ_I, respectively. $\boldsymbol{\sigma}_f^{FSI}$ and $\boldsymbol{\sigma}_s^{FSI}$ represent Cauchy stress of fluid and structure at the interface, respectively. $\mathbf{n}_f$ and $\mathbf{n}_s$ are outer normal unit vector of fluid and structure, respectively, $\mathbf{n}_s = -\mathbf{n}_f$.

To enforce the boundary conditions on the fluid-structure interface, a Lagrange multiplier is introduced for Dirichlet boundary condition (Badia *et al*. 2008a, b). Thus, a Lagrange multiplier is introduced into Eq. (1), which can be written as the following weighted residual form

$$\delta_{\mathrm{I}} = \int_{\Gamma I} (\mathbf{u}_{ES}(\vartheta_{\Gamma I}^1(\lambda), \vartheta_{\Gamma I}^2(\lambda), \vartheta_{\Gamma I}^3(\lambda) - \mathbf{u}_I(\lambda)) \cdot \Theta \left| \frac{d\mathbf{u}_{ES}(\vartheta_{\Gamma I}^1(\lambda), \vartheta_{\Gamma I}^2(\lambda), \vartheta_{\Gamma I}^3(\lambda))}{d\lambda} \right| d\lambda \tag{4}$$

where Θ is Lagrange multiplier, which can be regarded as the surface traction imposed on the interface Γ_I for the sake of generating the required boundary deformation.

2.3 Discretization of the governing equations

To obtain strongly coupled simultaneous equations, discretization of the fluid, structural and linear elastic governing equations both in time and space is required. The governing equations of the fluid, structure and linear elastic model are discretized with Galerkin finite element methods in space. Implicit finite difference methods are employed for time discretization. The discretization can be regarded as the process for obtaining the weak forms of the equations through weighted residual method.

The fluid is considered as an incompressible viscous flow and governed by the Navier–Stokes equations. Thus, the governing equations, i.e., continuity and momentum equations in the fluid domain Ω^f can be written as:

$$\nabla \cdot \mathbf{v}_f = 0 \quad \text{in } \Omega^f \tag{5}$$

$$\rho_f \left(\frac{\partial \mathbf{v}_f}{\partial t} + \mathbf{v}_f \cdot \nabla \mathbf{v}_f \right) = \nabla \cdot \boldsymbol{\sigma}^f \quad \text{in } \Omega^f \tag{6}$$

where $\mathbf{v}_f$ stands for fluid velocity, ρ_f is fluid density, $\boldsymbol{\sigma}^f$ is the stress tensor, $\boldsymbol{\sigma}^f = \mu[\nabla \mathbf{v}_f + (\nabla \mathbf{v}_f)^T] - p\mathbf{E}$, μ is the fluid viscosity, $\mathbf{E}$ stands for unit matrix, p is the fluid pressure.

The weighted residual form of the fluid continuity and momentum equations are referred in Sun and Gu (2014).

The governing equations for the structure are described by a total Lagrange (T.L.) formulation and a large deformation theory. The weighted residual form of the structure governing equations in the material point can be written as

$$-\int_{\Omega_0^s} (\eta \cdot \mathbf{b}_s \cdot \delta \mathbf{u}_s(\vartheta^i) - \eta : (\delta \mathbf{u}_s(\vartheta^i) d\Omega + \int_{\Gamma_{N0}^S \cup \Gamma_{I0}} ((\eta \cdot \mathbf{n}_s^0) : (\cdot \delta \mathbf{u}_s(\vartheta^i) d\Gamma = 0 \tag{7}$$

where η is test function, chosen as piecewise polynomial function, Ω_s^0 denotes initial

configuration of the structure domain, Γ^s_{N0} and Γ_{I0} represent initial Neumann boundary and initial configuration at the interface, respectively, $\mathbf{b}_s$ denotes the volume force of the structure, $\mathbf{u}_s$ denotes displacement of the structure, $\mathbf{n}^0_s$ is the initial outer normal unit vector of structure.

For data transfer on the fluid-structure interface, linear elastic model is introduced to deal with the deformation of the fluid. Considering the boundary conditions at the interface with Lagrange multiplier introduced earlier, Lagrange multiplier is introduced into linear elastic model accordingly. The weighted residual form of the linear elastic model in the material point form can be written as

$$-\int_{\Omega^s_0}(\eta:((\Theta^2\frac{\partial^2\mathbf{u}_{LE}}{\partial t^2})\cdot\delta\mathbf{u}_{LE}(\vartheta^i))d\Omega+\int_{\Gamma^S_{N0}\cup\Gamma_{I0}}((\eta\cdot\mathbf{n}^0_s):((\Theta^2\frac{\partial^2\mathbf{u}_{LE}}{\partial t^2})\cdot\delta\mathbf{u}_{LE}(\vartheta^i))d\Gamma=0 \quad (8)$$

where Θ is Lagrange multiplier, $\Theta=(L/T)\sqrt{(\rho_S E/\boldsymbol{\sigma}_p)}$, Θ^2 could be regarded as dimensional value of structure density, L and T are dimensional value of space and time coordinates, $\boldsymbol{\sigma}_p$ is 2nd Piola-Kirchhoff stress tensor, $\boldsymbol{\chi}_{LE}$ denotes displacement of the linear elastic model.

The weighted residual form of coupling condition (3) can be written as

$$\int_{\Gamma_{I0}}\eta\cdot\boldsymbol{\sigma}_s(\mathbf{u}_I(\lambda)\cdot\mathbf{n}^s_0)d\Gamma+\int_{\Gamma_{I1}}\zeta\cdot\boldsymbol{\sigma}_f(\mathbf{u}_I(\lambda))\cdot\mathbf{n}_f d\Gamma=0 \quad (9)$$

where the first term represents the structure contribution on the initial configuration, the second term stands for the fluid contribution on the deformed mesh.

One-step-θ temporal discretization is employed to get the discretization form of the coupling condition (2), which can be written as

$$\mathbf{v}_f^{n+1}=\frac{1}{\theta}\frac{d\mathbf{d}^{\mathbf{u},n+1}_{\Gamma_I}-d\mathbf{d}^{\mathbf{u},n}_{\Gamma_I}}{dt}-\frac{1-\theta}{\theta}\mathbf{v}_f^n \quad (10)$$

where $1/2\le\theta\le1$ (Förster *et al*. 2005)

The relationship of displacement of linear elastic model and fluid velocity can be written as

$$\mathbf{u}^{n+1}_{LE}=\mathbf{u}^n_{LE}+\theta\Delta t\mathbf{v}_f^{n+1}+(1-\theta)\Delta t\mathbf{v}_f^n \quad (11)$$

Then the simultaneous equations based on linear elastic model and Lagrange multiplier can be written as

$$\mathbf{f}_F=\int_{\Omega^f}(\omega\nabla\cdot\mathbf{v}_f-\zeta\cdot\rho_f(\frac{\partial\mathbf{v}_f}{\partial t}+\mathbf{v}_f\cdot\nabla\mathbf{v}_f)+\boldsymbol{\sigma}^f:\nabla\zeta)d\Omega=0 \quad (12)$$

$$\mathbf{f}_S=\int_{\Omega^0_s}(\eta\cdot\mathbf{b}_s\cdot\delta\mathbf{u}_s(\vartheta^i)-\eta:(\delta\mathbf{u}_s(\vartheta^i))d\Omega=0 \quad (13)$$

$$\mathbf{f}_{LE}=\int_{\Omega^0_s}(\eta:((\Theta^2\frac{\partial^2\mathbf{u}_{LE}}{\partial t^2})\cdot\delta\mathbf{u}_{LE}(\vartheta^i))d\Omega=0 \quad (14)$$

$$\mathbf{f}_F^{FSI} = \int_{\Gamma_I} \zeta \cdot \boldsymbol{\sigma}_f(\mathbf{u}_I(\lambda)) \cdot \mathbf{n}_f d\Gamma = 0 \tag{15}$$

$$\mathbf{f}_S^{FSI} = \int_{\Gamma_{I0}} ((\eta \cdot \mathbf{n}_0^s) \cdot \boldsymbol{\sigma}_s(\mathbf{u}_I(\lambda)) d\Gamma = 0 \tag{16}$$

where $\mathbf{f}_F$, $\mathbf{f}_S$ and $\mathbf{f}_{LE}$ denote weighted residual form of the fluid, solid and linear elastic model equations, respectively, $\mathbf{f}_F^{FSI}$ and $\mathbf{f}_S^{FSI}$ represent weighted residual form of the coupling conditions at the interface, ω and ζ denote test functions, which are chosen as pressure shape functions and velocity shape functions in local coordinates, respectively, Ω stands for spatial domain composed of Dirchlet boundary Γ_D, Neumann boundary Γ_N and fluid-structure interface Γ_I , Γ_N^f represents the fluid Neumann boundary. The unknowns of the simultaneous equations are the fluid velocity $\mathbf{v}_f$, fluid pressure $\mathbf{p}$, linear elastic model displacement $\mathbf{u}_{LE}$ and structural displacement $\mathbf{u}_s$.

3. Solution approach

The nonlinear strongly coupled simultaneous equations derived above need to be solved in one time step, after Newton linearization which can be written as

$$\frac{d\mathbf{f}_{FSI}}{d\mathbf{x}} \Delta\mathbf{x}_i = -\mathbf{f}_{FSI}^i \tag{17}$$

Where $\mathbf{f}_{FSI}$ stands for the above simultaneous equations, $\mathbf{x}$ represents all the unknowns in the equations, $\mathbf{J}^{FSI} = \dfrac{d\mathbf{f}_{FSI}}{d\mathbf{x}}$ is Jacobian matrix, $\mathbf{i}$ stands for iterative time step.

In the work here, block preconditioners are proposed considering the convenience and computation efficiency. Their application requires efficient sub-block solvers. Thus, considering Lagrange multiplier, Eq. (17) after Newton linearization can be written in the following block form as

$$\begin{bmatrix} \dfrac{\partial \mathbf{f}_S}{\partial \mathbf{u}_s} & \delta \dfrac{\partial \mathbf{f}_S}{\partial \mathbf{u}_s^{FSI}} & & & \\ \dfrac{\partial \mathbf{f}_S^{FSI}}{\partial \mathbf{u}_s} & \delta\left(\dfrac{\partial \mathbf{f}_S^{FSI}}{\partial \mathbf{u}_s^{FSI}} + \dfrac{\partial \mathbf{f}_F^{FSI}}{\partial \mathbf{u}_{LE}^{FSI}}\right) + \dfrac{\partial \mathbf{f}_F^{FSI}}{\partial \mathbf{v}_f^{FSI}} & \dfrac{\partial \mathbf{f}_F^{FSI}}{\partial \mathbf{v}_f} & & \\ & \delta \dfrac{\partial \mathbf{f}_F}{\partial \mathbf{u}_{LE}^{FSI}} + \dfrac{\partial \mathbf{f}_F}{\partial \mathbf{v}_f^{FSI}} & \dfrac{\partial \mathbf{f}_F}{\partial \mathbf{v}_f} & \dfrac{\partial \mathbf{f}_F}{\partial \mathbf{u}_{LE}} & \\ & & & \delta \dfrac{\partial \mathbf{f}_{LE}}{\partial \mathbf{u}_{LE}^{FSI}} & \left(\dfrac{\partial \mathbf{f}_{LE}}{\partial \mathbf{u}_{LE}} + \Theta \dfrac{\partial \mathbf{f}_F}{\partial \mathbf{u}_{LE}} + \delta \dfrac{\partial \mathbf{f}_F^{FSI}}{\partial \mathbf{u}_{LE}^{FSI}}\right) \\ & & \left(\dfrac{\partial \mathbf{f}_{LE}}{\partial \mathbf{u}_{LE}} + \delta \dfrac{\partial \mathbf{f}_F}{\partial \mathbf{u}_{LE}^{FSI}} + \Theta \dfrac{\partial \mathbf{f}_F^{FSI}}{\partial \mathbf{u}_{LE}}\right) & & \end{bmatrix} \begin{bmatrix} \Delta \mathbf{u}_s^i \\ \Delta \mathbf{v}_{*f}^{FSI,i} \\ \Delta \mathbf{v}_{*f}^i \\ \Delta \mathbf{u}_{LE}^i \\ \Theta \Delta \mathbf{u}_{LE}^i \end{bmatrix} = -\mathbf{f}_{FSI}^i \tag{18}$$

where $\mathbf{v}_{*f}$ represents all the unknowns of the fluid domain, including fluid velocity and pressure, $\mathbf{v}_{*f}^{FSI}$ stands for the fluid unknowns on the interface, $\delta = \theta\Delta t$, $\Theta\Delta\mathbf{u}_{LE}$ denotes unknown linear elastic model displacement with discretized Lagrange multiplier imposed on the fluid-structure interface.

For convenience, the Jacobian matrix of linear algebraic system of Eq. (18) can be written as

$$\mathbf{J}^{FSI} = \begin{pmatrix} \mathbf{D}_s^S & \delta\mathbf{D}_{sFSI}^S & & & \\ \mathbf{D}_s^{SFSI} & \delta(\mathbf{D}_{sFSI}^{SFSI} + \mathbf{D}_{LEFSI}^{FFSI}) + \mathbf{U}_{fFSI}^{FFSI} & \mathbf{U}_f^{FFSI} & & \\ & \delta\mathbf{D}_{LEFSI}^F + \mathbf{U}_{fFSI}^F & \mathbf{U}_f^F & \mathbf{D}_{LE}^F & \\ & & & \delta\mathbf{D}_{LEFSI}^{LE} & (\mathbf{D}_{LE}^{LE} + \Theta\mathbf{D}_{LE}^F + \delta\mathbf{D}_{LEFSI}^{FFSI}) \\ & & & (\mathbf{D}_{LE}^{LE} + \delta\mathbf{D}_{LEFSI}^F + \Theta\mathbf{D}_{LE}^{FFSI}) & \end{pmatrix} \tag{19}$$

where $\mathbf{D} = \dfrac{\partial \mathbf{f}}{\partial \mathbf{u}}$ corresponding to each term in Eq. (18), the superscripts and subscripts keep uniformity with each term in Eq. (18) for distinguishing, $\mathbf{D}_{LE}^{LE} + \Theta\mathbf{D}_{LE}^F + \delta\mathbf{D}_{LEFSI}^{FFSI}$ and $\mathbf{D}_{LE}^{LE} + \delta\mathbf{D}_{LEFSI}^F + \Theta\mathbf{D}_{LE}^{FFSI}$ can be regarded as discretized gradient and operator, respectively, which indicate Lagrange multiplier has been imposed to enforce the boundary condition (1) and the effects of the structure displacement on the linear elastic model displacement, i.e., $\mathbf{D}_{LE}^{LE} + \Theta\mathbf{D}_{LE}^F + \delta\mathbf{D}_{LEFSI}^{FFSI} = (\mathbf{D}_{LE}^{LE} + \delta\mathbf{D}_{LEFSI}^F + \Theta\mathbf{D}_{LE}^{FFSI})^T$.

4. Preconditioning technique

Generalized minimal residual method (Saad 2003) with preconditioning can be employed to solve Eq. (17). GMRES is a Krylov subspace projection method for solving large non-symmetric linear equations. Preconditioning technique is usually needed for the GMRES to accelerate the convergence. Preconditioning technique is to diminish computation time for solving the linearized equations through accumulating eigenvalues of linear iteration matrix. The preconditioner $\mathbf{M}_{LE}^{PR}$ for linear elastic model equation is firstly presented, and the preconditioner $\mathbf{M}_{FSI}^{PR}$ for simultaneous equations is proposed.

4.1 Reformulation of the linear elastic model as a saddle point problem

To obtain preconditioning matrix of the linear elastic model and fluid-structure system, the fluid nodes are considered as material points to ensure the discretized fluid equations not directly correlated to real structure deformation, and the linear elastic model not directly correlated to the fluid. Thus, special blocked structure could be utilized in the Jacobian matrix to modularize the preconditioning matrix and to use it repeatedly in the computation.

Firstly, preconditioner of the linear elastic model is derived by reformulating its linearized equations as a saddle point problem. Any non-linear equations after linearization, if properly

blocked, could be reformulated as saddle point problems (Farhat and Vinod 2014, Lazarov and Sigmund 2011). Thus, the linear elastic model of Eq. (14), after linearization by the Newton-Rapshon method, can be written as the following saddle point problem

$$\mathbf{Au}=\mathbf{b} \tag{20}$$

i.e.

$$\mathbf{J}^{LE}\Delta\mathbf{x}=\begin{pmatrix}\mathbf{A}_{LE} & \mathbf{B}^{T}\\ \mathbf{B} & 0\end{pmatrix}\begin{pmatrix}\Delta\mathbf{u}_{LE}\\ \Theta\Delta\mathbf{u}_{LE}\end{pmatrix}=\mathbf{-f}_{\mathrm{LE}} \tag{21}$$

where $\mathbf{A}_{LE}=\delta\mathbf{D}_{LEFSI}^{LE}$ corresponds to the equilibrium state of the system and thus symmetric definite positive, $\mathbf{B}$ is a full-rank $n\times m(m\geq n)$ diagonal matrix, whose discretization was shown to be steady in Farhat and Vinod (2014),

$\mathbf{B}^{T}=(\mathbf{D}_{LE}^{LE}+\Theta\mathbf{D}_{LE}^{F}+\delta\mathbf{D}_{LEFSI}^{FFSI})$, $\mathbf{B}=(\mathbf{D}_{LE}^{LE}+\delta\mathbf{D}_{LEFSI}^{F}+\Theta\mathbf{D}_{LE}^{FFSI})$.

Iterative method is employed to solve Eq. (21). A preconditioner $\mathbf{P}$ is usually introduced to solve Eq. (21), and left preconditioner is adopted here, i.e.

$$\mathbf{P}^{-1}\mathbf{Au}=\mathbf{P}^{-1}\mathbf{b} \tag{22}$$

Based on preconditioning matrix proposed by Rees and Greif (2007), considering characteristics of the strongly coupled simultaneous equations here, preconditioner of Eq. (21) can be written as the following blocked triangle matrix form

$$\mathbf{M}_{LE}^{PR}=\begin{pmatrix}\mathbf{A}_{LE}+\mathbf{B}^{T}\mathbf{W}^{-1}\mathbf{B} & \mathbf{kB}^{T}\\ & \mathbf{W}\end{pmatrix} \tag{23}$$

where $\mathbf{W}\in R^{n}\times R^{n}$ is symmetric definite positive, which can be chosen arbitrarily in order to construct the effective preconditioner, $\mathbf{k}$ is a scalar factor, which designed to adjust the computation convergence through effects of different values on GMRES iteration and relative residuals. In order to guarantee all the eigenvalues of the preconditioner to be bounded, $\mathbf{k}$ should be real among proper value. (Rees and Greif 2007). In the work here, $\mathbf{k}$ is an important factor, whose proper values and implicancies it may have will be discussed in detail through the following computation cases.

Based on the above requirements, $\mathbf{W}$ in this work is chosen as

$$\mathbf{W}=\gamma\mathbf{E}=\begin{pmatrix}\gamma\mathbf{E}_{x} & & \\ & \gamma\mathbf{E}_{y} & \\ & & \gamma\mathbf{E}_{z}\end{pmatrix} \tag{24}$$

where $\gamma=\|\mathbf{A}_{LE}\|_{\infty}$, $\mathbf{E}$ stands for unit matrix.

Combing Eqs. (23) and (24), along the coordinate, the unknown linear elastic model displacement is divided into unknown nodal vector on the interface and not on the interface. Then an initial preconditioner of the linear elastic model can be obtained as

$$\mathbf{M}_{LE}^{PR}=\begin{bmatrix}
\mathbf{A}_{xx} & \mathbf{A}_{x\bar{x}} & \mathbf{A}_{xy} & \mathbf{A}_{x\bar{y}} & \mathbf{A}_{xz} & \mathbf{A}_{x\bar{z}} & & & \\
\mathbf{A}_{\bar{x}x} & \mathbf{A}_{\bar{x}\bar{x}}+\gamma\mathbf{E} & \mathbf{A}_{\bar{x}y} & \mathbf{A}_{\bar{x}\bar{y}} & \mathbf{A}_{\bar{x}z} & \mathbf{A}_{\bar{x}\bar{z}} & \mathbf{kZ}_x & & \\
\mathbf{A}_{yx} & \mathbf{A}_{y\bar{x}} & \mathbf{A}_{yy} & \mathbf{A}_{y\bar{y}} & \mathbf{A}_{y\bar{z}} & \mathbf{A}_{y\bar{z}} & & & \\
\mathbf{A}_{\bar{y}x} & \mathbf{A}_{\bar{y}x} & \mathbf{A}_{\bar{y}y} & \mathbf{A}_{\bar{y}\bar{y}}+\gamma\mathbf{E} & \mathbf{A}_{\bar{y}z} & \mathbf{A}_{\bar{y}\bar{z}} & & \mathbf{kZ}_y & \\
\mathbf{A}_{zx} & \mathbf{A}_{z\bar{x}} & \mathbf{A}_{zy} & \mathbf{A}_{z\bar{y}} & \mathbf{A}_{zz} & \mathbf{A}_{z\bar{z}} & & & \mathbf{kZ}_z \\
\mathbf{A}_{\bar{z}x} & \mathbf{A}_{\bar{z}x} & \mathbf{A}_{\bar{z}y} & \mathbf{A}_{\bar{z}\bar{y}} & \mathbf{A}_{\bar{z}z} & \mathbf{A}_{\bar{z}\bar{z}}+\gamma\mathbf{E} & & & \\
 & & & & & & \gamma\mathbf{E} & &
\end{bmatrix} \tag{25}$$

where $\mathbf{A}=\mathbf{A}_{LE}+\mathbf{B}^T\mathbf{W}^{-1}\mathbf{B}$, subscripts $\mathbf{x},\mathbf{y},\mathbf{z}$ and $\bar{\mathbf{x}},\bar{\mathbf{y}},\bar{\mathbf{z}}$ are unknown displacement nodal vectors and unknown displacement nodal vectors constrained by Lagrange multiplier of the linear elastic model, respectively. $\left|\mathbf{Z}_x\right|_{mn}=\left|\mathbf{Z}_y\right|_{mn}=\left|\mathbf{Z}_z\right|_{mn}=\int_{\Gamma I}\bar{\alpha}_m\bar{\alpha}_n d\Omega$, $\bar{\alpha}_m$ and $\bar{\alpha}_n$ are basis functions on the fluid-structure interface, which are chosen as polynomial function relevant to geometric positions of the fluid mesh nodes.

The spectral properties of the preconditioner can be referred in Rees and Greif (2007). It was pointed out by Rees and Greif (2007) that, when $\mathbf{k}=-1$, there were $(m-n)$ eigenvalues for preconditioner $\mathbf{M}_{LE}^{PR}$ and there were p eigenvalues $\phi_{\pm}=\frac{1\pm\sqrt{5}}{2}$, while the rest eigenvalues fell between $(\frac{1-\sqrt{5}}{2},0)\cup(1,\frac{1+\sqrt{5}}{2})$.

To further improve the computation efficiency, Eq. (25) is further simplified. Blocked preconditioner (Geuzaine and Remacle 2009) is adopted by substituting $\mathbf{A}_{LE}+\mathbf{B}^T\mathbf{W}^{-1}\mathbf{B}$ with the upper triangle block of $\mathbf{A}_{LE}+\mathbf{B}^T\mathbf{W}^{-1}\mathbf{B}$, then we obtain the modified preconditioner of the linear elastic model,

$$\tilde{\mathbf{M}}_{LE}^{PR}=\begin{bmatrix}
\mathbf{A}_{xx} & \mathbf{A}_{x\bar{x}} & \mathbf{A}_{xy} & \mathbf{A}_{x\bar{y}} & \mathbf{A}_{xz} & \mathbf{A}_{x\bar{z}} & & & \\
\mathbf{A}_{\bar{x}x} & \mathbf{A}_{\bar{x}\bar{x}}+\gamma\mathbf{E} & \mathbf{A}_{\bar{x}y} & \mathbf{A}_{\bar{x}\bar{y}} & \mathbf{A}_{\bar{x}z} & \mathbf{A}_{\bar{x}\bar{z}} & \mathbf{kZ}_x & & \\
 & & \mathbf{A}_{yy} & \mathbf{A}_{y\bar{y}} & \mathbf{A}_{y\bar{z}} & \mathbf{A}_{y\bar{z}} & & & \\
 & & \mathbf{A}_{\bar{y}y} & \mathbf{A}_{\bar{y}\bar{y}}+\gamma\mathbf{E} & \mathbf{A}_{\bar{y}z} & \mathbf{A}_{\bar{y}\bar{z}} & & \mathbf{kZ}_y & \\
 & & & & \mathbf{A}_{zz} & \mathbf{A}_{z\bar{z}} & & & \mathbf{kZ}_z \\
 & & & & \mathbf{A}_{\bar{z}z} & \mathbf{A}_{\bar{z}\bar{z}}+\gamma\mathbf{E} & & & \\
 & & & & & & \gamma\mathbf{E} & &
\end{bmatrix} \tag{26}$$

For the above preconditioner, the following diagonal blocked subsystems are utilized for calculation.

$$\mathbf{A}_1=\begin{pmatrix}\mathbf{A}_{xx} & \mathbf{A}_{x\bar{x}}\\ \mathbf{A}_{\bar{x}x} & \mathbf{A}_{\bar{x}\bar{x}}+\gamma\mathbf{E}\end{pmatrix},\ \mathbf{A}_2=\begin{pmatrix}\mathbf{A}_{yy} & \mathbf{A}_{\bar{x}\bar{y}}\\ \mathbf{A}_{\bar{y}y} & \mathbf{A}_{\bar{y}\bar{y}}+\gamma\mathbf{E}\end{pmatrix},\ \mathbf{A}_3=\begin{pmatrix}\mathbf{A}_{zz} & \mathbf{A}_{z\bar{z}}\\ \mathbf{A}_{\bar{z}z} & \mathbf{A}_{\bar{z}\bar{z}}+\gamma\mathbf{E}\end{pmatrix} \tag{27}$$

4.2 Preconditioner of the fluid-structure interaction system

Substituting the lower right block in Eq. (19) with the proposed preconditioning matrix of the linear elastic model, i.e., Eq. (23), yields fluid-structure interaction system preconditioner for the simultaneous equations (referred as FSI preconditioner hereafter) as follows

$$\mathbf{M}_{FSI}^{PR}=\begin{pmatrix} \mathbf{D}_s^S & \delta\mathbf{D}_{sFSI}^S & & & \\ \mathbf{D}_s^{SFSI} & \delta(\mathbf{D}_{sFSI}^{SFSI}+\mathbf{D}_{LEFSI}^{FFSI})+\mathbf{U}_{fFSI}^{FFSI} & \mathbf{U}_f^{FFSI} & & \\ & \delta\mathbf{D}_{LEFSI}^F+\mathbf{U}_{fFSI}^F & \mathbf{U}_f^F & \mathbf{D}_{LE}^F & \\ & & & \mathbf{A}_{LE}+\mathbf{B}^T\mathbf{W}^{-1}\mathbf{B} & \mathbf{k}\mathbf{B}^T \\ & & & & \mathbf{W} \end{pmatrix} \tag{28}$$

Initial and modified FSI preconditioner can be obtained by employing the linear elastic model preconditioner, Eqs. (25) and (26) to calculate Eq. (28), respectively.

To validate preconditioning matrix (28), spectral characteristics of $(M^{FSI})^{-1}J^{FSI}$ should be analyzed. To this end, Jacobian matrix in Eq. (19) is rewritten in the following diagonal block form as

$$\mathbf{J}^{FSI}=\begin{pmatrix} \mathbf{J}_{11} & \\ & \mathbf{J}_{22} \end{pmatrix}=\begin{pmatrix} \mathbf{D}_s^S & \delta\mathbf{D}_{sFSI}^S & & & & \\ \mathbf{D}_s^{SFSI} & \delta(\mathbf{D}_{sFSI}^{SFSI}+\mathbf{D}_{LEFSI}^{FFSI})+\mathbf{U}_{fFSI}^{FFSI} & \mathbf{U}_f^{FFSI} & & & \\ & \delta\mathbf{D}_{LEFSI}^F+\mathbf{U}_{fFSI}^F & \mathbf{U}_f^F & \mathbf{D}_{LEl}^F & \mathbf{D}_{LEq}^F & \\ & & & \mathbf{A}_{ll} & \mathbf{A}_{lq} & \\ & & & \mathbf{A}_{ql} & \mathbf{A}_{qq} & \mathbf{k}\mathbf{Z} \\ & & & & \mathbf{k}\mathbf{Z} & \end{pmatrix} \tag{29}$$

where $\mathbf{J}_{11}=\begin{pmatrix} \mathbf{D}_s^S & \delta\mathbf{D}_{sFSI}^S & \\ \mathbf{D}_s^{SFSI} & \delta(\mathbf{D}_{sFSI}^{SFSI}+\mathbf{D}_{LEFSI}^{FFSI})+\mathbf{U}_{fFSI}^{FFSI} & \mathbf{U}_f^{FFSI} \\ & \delta\mathbf{D}_{LEFSI}^F+\mathbf{U}_{fFSI}^F & \mathbf{U}_f^F \end{pmatrix}$, $\mathbf{J}_{22}=\begin{pmatrix} \mathbf{D}_{LEl}^F & \mathbf{D}_{LEq}^F & \\ \mathbf{A}_{ll} & \mathbf{A}_{lq} & \\ \mathbf{A}_{ql} & \mathbf{A}_{qq} & \mathbf{k}\mathbf{Z} \\ & \mathbf{k}\mathbf{Z} & \end{pmatrix}$,

$$\mathbf{A}_{\mathrm{lq}}=\begin{pmatrix} \mathbf{A}_{x\bar{x}} & \mathbf{A}_{x\bar{y}} & \mathbf{A}_{x\bar{z}} \\ \mathbf{A}_{y\bar{x}} & \mathbf{A}_{y\bar{y}} & \mathbf{A}_{y\bar{z}} \\ \mathbf{A}_{z\bar{x}} & \mathbf{A}_{z\bar{y}} & \mathbf{A}_{z\bar{z}} \end{pmatrix},\quad \mathbf{A}_{\mathrm{ql}}=\begin{pmatrix} \mathbf{A}_{\bar{x}x} & \mathbf{A}_{\bar{x}y} & \mathbf{A}_{\bar{x}z} \\ \mathbf{A}_{\bar{y}x} & \mathbf{A}_{\bar{y}y} & \mathbf{A}_{\bar{y}z} \\ \mathbf{A}_{\bar{z}x} & \mathbf{A}_{\bar{z}y} & \mathbf{A}_{\bar{z}z} \end{pmatrix},\quad \mathbf{A}_{qq}=\begin{pmatrix} \mathbf{A}_{\bar{x}\bar{x}} & \mathbf{A}_{\bar{x}\bar{y}} & \mathbf{A}_{\bar{x}\bar{z}} \\ \mathbf{A}_{\bar{y}\bar{x}} & \mathbf{A}_{\bar{y}\bar{y}} & \mathbf{A}_{\bar{y}\bar{z}} \\ \mathbf{A}_{\bar{z}\bar{x}} & \mathbf{A}_{\bar{z}\bar{y}} & \mathbf{A}_{\bar{z}\bar{z}} \end{pmatrix},$$

subscripts q and l denote unknown nodal vector constrained by displacement and not constrained by displacement, respectively. There are n_v unknown nodal vector in the first row of $\mathbf{J}^{FSI}$, n_u unknown nodal vector in the second row, (n_c-n_d) unknown nodal vector in the third row, n_d discretized unknown Lagrange multiplier in fifth and sixth row, respectively.

Then preconditioner Eq. (28) can be written as

$$\mathbf{M}^{FSI} = \begin{pmatrix} \mathbf{J}_{11} & \mathbf{0} \\ \mathbf{0} & \mathbf{J}_{22} + \mathbf{\Xi} \end{pmatrix} \tag{30}$$

$$\mathbf{\Xi} = \begin{pmatrix} \gamma\mathbf{E} & \mathbf{k} \\ -\mathbf{Z} & \gamma\mathbf{E} \end{pmatrix} \tag{31}$$

Matrix $(\mathbf{M}^{FSI})^{-1}\mathbf{J}^{FSI}$ can be written as

$$(\mathbf{M}^{FSI})^{-1}\mathbf{J}^{FSI} = \begin{pmatrix} \mathbf{E} & \\ & (\mathbf{J}_{22} + \mathbf{\Xi})^{-1}\mathbf{J}_{22} \end{pmatrix} \tag{32}$$

where $(\mathbf{J}_{22} + \mathbf{\Xi})^{-1}\mathbf{J}_{22}$ can be regarded as Schur complement correlated to block $\mathbf{J}_{22}$, unit matrix $\mathbf{E}$ in the upper left block indicates that preconditioning matrix $(\mathbf{M}^{FSI})^{-1}\mathbf{J}^{FSI}$ at least contains $(n_v + n_u + n_c - n_d)$ unit eigenvalues, the rest $2n_d$ eigenvalues would be determined from spectrum of $(\mathbf{J}_{22} + \mathbf{\Xi})^{-1}\mathbf{J}_{22}$.

5. Procedures for simultaneous solutions with the preconditioning technique

The computer configuration is: Intel i7, memory capacity of DDR3 8GB. Based on circular GMRES algorithm (Barker and Cai 2010), procedures for simultaneous solutions with preconditioner proposed above are summarized as follows.

(1) Start iteration from a zero initial field for all variables in the equations for 2 to 3 step consecutive iterations to ensure convergence of Newton's Method. Implicitly treat the boundary conditions and loads at the interface of the entire fluid-structure interaction system. All the fluid variables were saved on the mesh nodes.

(2) Newton-Raphson method is employed to linearize the simultaneous equations to obtain linearized equations $\mathbf{A}\cdot\mathbf{x} = \mathbf{b}$. Left preconditioner and GMRES method is employed to solve the equations. The details are as follows.

(3) Randomly select initial estimate value x_0 and determine Krylov subspace dimension m. Define matrix $H_m \in R^{(m+1)\times m}$,where $H_m \in R^{(m+1)\times m}$ is upper Hessenberg matrix, $R^{(m+1)\times m}$ denotes space composed of all $(m+1)\times m$ matrices. Initialize the entries h_{ij} of H_m to be zero.

(4) Select m as a proper value, and start executing Arnoldi procedures, i.e.,

a Compute $\boldsymbol{\psi}_\mathbf{0} = \mathbf{b} - \mathbf{A}\mathbf{x}_0$, $\Pi = \|\boldsymbol{\psi}_\mathbf{0}\|_2$, $\boldsymbol{\psi}_\mathbf{1} = \boldsymbol{\psi}_\mathbf{0}/\beta$,where $\|\bullet\|_2$ stands for 2 norm of a vector or matrix.

b Compute $\mathbf{c}_j = \mathbf{A}\boldsymbol{\psi}_j$, $\mathbf{q} = (\mathbf{M}^{FSI})^{-1}\mathbf{c}_j (j = 1, 2\ldots, m)$, $\mathbf{c}$ stands for cost functions.

c Compute $\begin{cases} \mathbf{p}_{ij} = (\mathbf{q}, \boldsymbol{\psi}_i) \\ \mathbf{q} = \mathbf{q} - \mathbf{p}_{ij}\boldsymbol{\psi}_i \end{cases} (i = 1, 2\ldots, j)$, $\mathbf{p}_{j+1,j} = \|\mathbf{c}\|_2, \boldsymbol{\psi}_{j+1} = \mathbf{q}/\mathbf{p}_{j+1,j}$, and define a group of

orthogonal basis in Krylov subspace $\mathbf{C}_m = [\mathbf{c}_1, \mathbf{c}_2, \ldots, \mathbf{c}_m]$

(5) Compute $\mathbf{x}_m = \mathbf{x}_0 + \mathbf{C}_m \mathbf{y}_m$, and $\mathbf{y}_m = \arg\min \left\| \alpha \boldsymbol{\psi}_1 - \mathbf{H}_m \mathbf{y}_m \right\|$, which represents the minimized residual normed vectors of cost functions.

(6) When $\left\| \mathbf{b} - \mathbf{A}\mathbf{x}_m \right\| \le \varepsilon$, stop iteration ($\varepsilon$ is prescribed error limit). Otherwise, set $\mathbf{x}_0 = \mathbf{x}_m$, and go back to step (5) to re-compute.

(7) Save the obtained solutions as multi-dimensional dynamic arrays, save and output the final displacement, pressure, velocity, etc. after all the time step cycles.

6 Numerical examples

6.1 Fluid-structure interaction of a two-dimensional membranous structure

Since the proposed numerical procedures has been validated in the previous work of Sun and Gu (2014), in this work the authors are more interesed in the evaluation of the proposed preconditioners for the fluid-structure interaction and no more new validation examples are presented.

To evaluate the performance of the proposed preconditioners (initial and modified ones) for the fluid-structure interaction system, fluid-structure interaction of a two-dimensional membranous structure is computed first. The membranous structure is constructed of elastic membranous roof bearing gravity and two vertical rigid supporting walls, as shown in Fig. 1. It should be noted that the simulation in this work does not represent the scales of any characteristic wind engineering problem, but it rather focuses on the improvements of computations through the implemented preconditioning technique. Thus, Reynolds number is set to be 1700, and turbulence is not considered here.

Computation domain size is set as 400m×100m. The fluid domain is discretized with elastic model elements, while the membrane is discretized with triangular finite elements. Slip boundary is adopted for upper wall of the fluid domain, and non-slip boundary for lower wall and fluid-structure interface. A fully developed outlet boundary condition is chosen as outflow boundary condition. To obtain steady fluid field at the initial stage of the simulation, the solution after simulation time of 60s is set as the initial condition. A grid-independence has been performed to ensure the accuracy of the numerical simulation. The largest mesh size in the following comparison is ensured to be grid-independence. And the results obtained with the smallest mesh in the following comparison and those with a mesh nearly one time finer are very close and the maximum relative deviation is less than 2%.

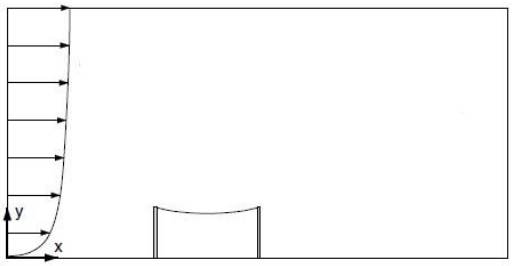

Fig. 1 Sketch of a two-dimensional membranous structure

Table 1 Average GMRES iteration numbers varying with mesh sizes for initial preconditioner

Mesh size h	Parameter $\mathbf{k}$			
	0.5	1	-1	8
1/23	19	19	19	19
1/46	21	21	21	21
1/69	22	22	22	22
1/92	24	24	24	24

Table 2 GMRES relative residuals varying with mesh sizes for the initial preconditioner

Mesh size h	Parameter $\mathbf{k}$			
	0.5	1	-1	8
1/23	7.627×10^{-6}	8.215×10^{-6}	8.234×10^{-6}	5.848×10^{-7}
1/46	5.652×10^{-6}	5.364×10^{-6}	6.735×10^{-6}	5.227×10^{-7}
1/69	5.323×10^{-6}	4.862×10^{-6}	5.347×10^{-6}	4.947×10^{-7}
1/92	4.967×10^{-6}	4.658×10^{-6}	5.269×10^{-6}	4.652×10^{-7}

A time step convergence study was conducted to find the largest time step compatible with the numerical scheme stability. This stability requires that the Courant number remains within some reasonably low limits. The time step is chosen in a way that the time discretization error and solution error are minimized. After comparison of results from several different Courant numbers and time steps, the greatest value of the time step was set to be 0.04. More than 8000 time steps correspond to about a 20 vortex shedding cycle. Iteration stops when relative residuals $\left\|\mathbf{b}-\mathbf{A}\mathbf{x}^{n}\right\|_{2}\le10^{-6}\left\|\mathbf{b}\right\|_{2}$. This convergence criterion is chosen to minimize the iteration errors.

Computation results are presented using preconditioner $(\mathbf{M}^{FSI})^{-1}\mathbf{J}^{FSI}$ with GMRES method. Average GMRES iteration numbers and relative residual varying with mesh sizes for different parameter k, by employing the initial FSI preconditioner, i.e., employing Eq. (25) to compute Eq. (28), are presented in Tables 1 and 2, respectively. The involved blocked matrices $\mathbf{V}$, $\mathbf{U}$, $\mathbf{S}+\mathbf{D}^{cd}\mathbf{W}^{-1}\mathbf{D}^{dc}$ and $\mathbf{W}$ are decomposed by LU method.

As shown in Tables 1 and 2,

(1) Average GMRES iteration times are not affected by the different k values for various mesh sizes, whereas GMRES relative residuals are affected. It was found during the computation that, the choice of $\mathbf{k}$ value, either positive or negative, will just affect the computation accuracy and has no specific implications for the computation. When $\mathbf{k}$ =8 the relative residuals are less than the prescribed tolerance, which suggests that the larger $\mathbf{k}$ value would accelerate the convergence. It is found that it was appropriate when $\mathbf{k}$ falls between [-1, 10] as real, and it is more accurate

when $\mathbf{k} \geq 8$.

(2) For the initial FSI preconditioner, variation of average GMRES iteration numbers (here average GMRES iteration numbers refers to computing the mean values of all the linear solutions whose GMRES convergence tolerance are 10^{-6} during Newton iteration) and relative residuals, with varying mesh sizes, are not obvious, which suggests that the initial preconditioner dependency on mesh is low. It also indicates that though the analysis of $(M^{FSI})^{-1} J^{FSI}$ eigenvalues is not complete previously, as the mesh refines, the maximum and minimum eigenvalue of $(M^{FSI})^{-1} J^{FSI}$ is bounded.

To compare computation efficiency, the modified FSI preconditioner, i.e., employing Eq. (26) to compute Eq. (28), is utilized for the computation, and the tolerance is set to be the same with that of the unmodified preconditioner. Average GMRES iteration numbers and relative residuals varying with mesh sizes are shown in Tables 3 and 4, respectively.

It can be seen from Table 3 and 4 that,

(1) For the modified FSI preconditioner, for different values of parameter $\mathbf{k}$, average GMRES iteration numbers for various mesh sizes are not affected, whereas GMRES relative residuals are affected, and the relative residuals become smaller when $\mathbf{k}$ becomes larger. The conclusion is consistent with that of the previous initial FSI preconditioner.

(2) It can be seen from Tables 3 and 4 that, for the modified FSI preconditioner, as the mesh refines, the average GMRES iteration numbers increase whereas GMRES relative residuals diminish.

Table 3 Average GMRES iteration numbers varying with mesh sizes for the modified preconditioner

Mesh size h	Parameter $\mathbf{k}$			
	0.5	1	-1	8
1/23	28	28	28	28
1/46	39	39	39	39
1/69	57	57	57	57
1/92	76	76	76	76

Table 4 GMRES relative residuals varying with mesh sizes for the modified preconditioner

Mesh size h	Parameter $\mathbf{k}$			
	0.5	1	-1	8
1/23	3.512×10^{-6}	$3..241\times10^{-6}$	3.645×10^{-6}	2.534×10^{-7}
1/46	$1..44\times10^{-6}$	1.027×10^{-6}	1.126×10^{-6}	1.956×10^{-7}
1/69	0.887×10^{-7}	0.812×10^{-7}	0.795×10^{-7}	4.365×10^{-8}
1/92	1.035×10^{-8}	1.123×10^{-8}	1.256×10^{-8}	6.234×10^{-9}

Table 5 Comparison of convergence with different FSI preconditioners

Method	Iteration numbers	Residuals	Computation time (Hours)
Without preconditioners	30	5.338×10^{-2}	59
Unmodified preconditioner	30	1.234×10^{-6}	39
Modified preconditioner	30	0.362×10^{-7}	31

(3) Results from the modified preconditioner is more sensitive to the mesh refinement, which indicates that the modified FSI preconditioner is more accurate than the initial one.

To further illustrate the efficiency, the convergence comparison is made between the initial and modified FSI preconditioner for the same iteration numbers (mesh size is 1/46，$\mathbf{k}$=8), as shown in Table 5.

It can be concluded from table 5 that, for the same iteration numbers, computation residuals without preconditioners are much larger than those with preconditioners. Besides, about 34% and 47% computation time are saved for the initial and modified FSI preconditioners, respectively. It is indicated that preconditioners greatly improve efficiency and accuracy in fluid-structure computation. It is found that, compared with the initial FSI preconditioner, residuals from the modified FSI preconditioner are much less, and about 20% computation time is saved, since the modified FSI preconditioner reduces the computation time for the linear sub-matrix blocks, resulting in the improving of accuracy and convergence.

Instantaneous pressure distribution contours at various time at specified parameters ($\mathbf{k}$=1, Θ=0) is given in Figs. 2(a)-2(d). It can be seen that the vortex sheds along the membrane leading edge, and forms a typical vortex street.

6.2 Fluid-structure interaction of a three-dimensional membranous structure

To verify the applicability of the proposed preconditioners, fluid-structure interaction of a three-dimensional membranous structure is also computed. Turbulence is not considered here for the priority is to evaluate the preconditioner performance. Fluid-structure interaction of a typical saddle membrane structure is computed using the proposed simultaneous method and preconditioners. The model and related parameters in computation are referred to in Sun and Gu (2014). Here the membranous structure rise f is taken as the dimensionless length, and (time) average inlet wind velocity is taken as the dimensionless velocity. When relative residuals $\left\|b-Ax^{n}\right\|_{2}\le10^{-5}\left\|b\right\|_{2}$, the iteration stops and the result is assumed to converge.

Table 6 shows the average GMRES iteration numbers and relative residual varying with mesh sizes for different parameter k (Θ=0，time t=200s), for the computation of the three-dimensional case when employing the modified FSI preconditioner.

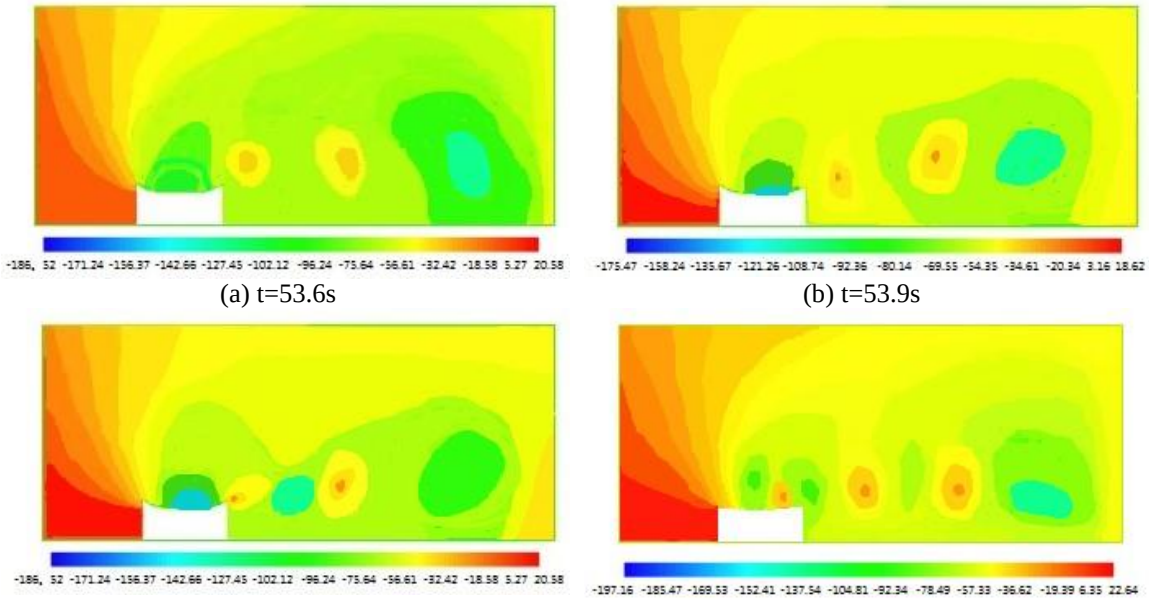

(a) t=53.6s (b) t=53.9s

(c) t=54.2s (d) t=54.6s

Fig. 2 Instantaneous pressure distribution at various time ($\mathbf{k}$ =0, Θ =0)

Table 6 Average GMRES iteration numbers varying with mesh sizes for the modified FSI preconditioner

Total mesh	Parameter $\mathbf{k}$			
(10 thousand)	0.5	1	-1	8
27	115	115	115	115
30	128	128	128	128
32	141	141	141	141
35	163	163	163	163

Through the analysis of data from Table 6, it can be concluded that, for different values of parameter k, average GMRES iteration numbers for various mesh sizes are not affected. In three-dimensional case, with the modified FSI preconditioner, the average iteration numbers increase as the mesh refinement increases, which indicates that the modified preconditioner is highly sensitive to the mesh refinement. The conclusion is consistent with that of the two-dimensional case. The preconditioners proposed is also validated in three-dimensional cases.

To illustrate the accuracy and efficiency of the preconditioner in three-dimensional FSI computation, comparison is made for GMRES relative residuals R_{GMRES} and computation time T_{GMRES} (hours) for various mesh numbers among the case without preconditioner, the initial FSI preconditioner, and modified FSI preconditioner, where k=1 , Θ =0. The results are shown in Table 7.

Table 7 Comparison of GMRES relative residuals and computation time (hour) for various mesh numbers using different preconditioners (Hours)

Total Mesh (10000)	without preconditioner		Initial preconditioner		Modified preconditioner	
	R_{GMRES}	T_{GMRES}	R_{GMRES}	T_{GMRES}	R_{GMRES}	T_{GMRES}
27	6.235×10^{-5}	102	3.356×10^{-5}	85	3.876×10^{-5}	68
30	5.234×10^{-5}	131	2.947×10^{-5}	94	1.324×10^{-5}	76
32	4.315×10^{-5}	154	2.245×10^{-5}	108	7.264×10^{-6}	89
35	4.198×10^{-5}	182	1.966×10^{-5}	127	3.214×10^{-6}	102

It can be concluded from Table 7 that,

(1) Without preconditioners, though relative residuals diminish gradually with the increase of mesh refinement (i.e., computation accuracy improving as mesh refines), computation time increase greatly. It is found that when mesh accuracy increases about 20%, the computation accuracy only improves about 3%, with the stability not affected, while the computation time increases about 30%. This shows that, without preconditioners, computation accuracy and stability is little affected as mesh refines.

(2) In the case of the initial FSI preconditioner, compared with the case without preconditioners, it saves about 30% computation time for the same computation accuracy. When the mesh accuracy improves about 20%, computation accuracy improves about 15% on average, and computation time increases about 20%. It is indicated that in the case of the initial FSI preconditioner, computation accuracy and efficiency are both greatly improved. On the other hand, as the mesh is refined, the relative residuals diminish not so obviously, which suggests that for the initial FSI preconditioner, the computation accuracy does not show a high dependency on mesh refinement, consistent with that of the two-dimensional case.

(3) In the case of the modified FSI preconditioner, it can be found that when mesh accuracy improves, GMRES relative residuals diminish greatly. When mesh accuracy improves about 20%, computation accuracy improves about 55% on average, and computation time only increases about 15%. It is indicated that for the modified FSI preconditioner, computation accuracy shows a fairly high dependency on mesh refinement, which is also verified in the two-dimensional case. It is verified once again the priority of the modified FSI preconditioner.

Since the time step is also among the key factors affecting the accuracy and efficiency in a fluid-structure interaction computation, the time-step effects of the modified FSI preconditioning matrix were analyzed. The effects of the Lagrange multiplier on the computation results were also analyzed. Table 8 gives the variation of GMRES iteration numbers N_{GMRES} and relative residuals R_{GMRES} with varying time steps and Lagrange multiplier.

It can be concluded from Table 8 that, the GMRES iterative numbers increase as time step increases, and decrease as the Lagrange multiplier increases. The GMRES residuals increase as the time step increases, but vary little as the Lagrange multiplier increases. This shows that the computation accuracy and efficiency become higher as the time step becomes smaller. Lagrange multiplier affects GMRES iterative numbers whereas affects residuals little. It can be concluded that time step is a decisive factor, whereas Lagrange multiplier is a much less influential factor.

Table 8 Variation of GMRES iteration numbers and relative residuals with varying time steps and Lagrange multiplier

time step Dt	0.025		0.050		0.075		0.100	
	N_{GMRES}	R_{GMRES}	N_{GMRES}	R_{GMRES}	N_{GMRES}	R_{GMRES}	N_{GMRES}	R_{GMRES}
Θ^2 =0.0	28.3	6.231×10^{-6}	30.4	7.452×10^{-6}	36.9	3.657×10^{-6}	41.2	6.543×10^{-5}
Θ^2 =0.6	26.1	4.342×10^{-6}	28.6	6.265×10^{-6}	33.8	2.053×10^{-6}	36.5	5.453×10^{-5}
Θ^2 =1.5	24.6	3.453×10^{-6}	26.4	4.341×10^{-6}	28.9	1.034×10^{-6}	32.6	4.237×10^{-5}
Θ^2 =15.0	19.3	1.984×10^{-6}	21.5	3.678×10^{-6}	23.4	8.765×10^{-5}	26.7	3.235×10^{-5}

Thus, the dimensionless parameters involved in Lagrange multiplier can be chosen just for the sake of convenience of computation.

7. Conclusions

A preconditioning technique, for a simultaneous solution to wind-membrane interaction, is presented. In the simultaneous equations, a linear elastic model was employed to deal with the fluid-structure data transfer at the interface. A Lagrange multiplier was introduced to impose the specified boundary conditions at the interface. An initial linear elastic model preconditioner and modified one were derived by treating the linearized elastic model equation as a saddle point problem. The FSI preconditioner for the simultaneous equations was then derived based on the initial and modified linear elastic model preconditioner. The wind-membrane interaction, for two- and three- dimensional membrane structures, were computed using the proposed preconditioners. The main conclusions are as follows:

- The value of k in the preconditioner has no effect on the average GMRES iteration numbers for various mesh sizes, whereas the value of k in the preconditioner affects the GMRES relative residuals. It is found that it was appropriate when k falls between [-1, 10] as real, and it is more accurate if $k \geq 8$.
- The computational efficiency with preconditioners is greatly improved compared with the case without a preconditioning matrix. The initial FSI preconditioning matrix dependency on mesh accuracy is lower than that of the modified FSI preconditioning matrix, which indicates that the priority of the modified FSI preconditioning matrix is computational accuracy. For the modified FSI preconditioning matrix, the computation residuals are much less than that of the initial one, and computation time also decreases. This is due to that, for the modified FSI preconditioning matrix, linear sub-matrix computations are diminished, resulting in the improvement of accuracy and efficiency.
- The computational accuracy and efficiency become higher as the time step becomes smaller. The Lagrange multiplier affects the GMRES iterative times, buts little affects the residuals. It

can be concluded that time step is a decisive factor whereas Lagrange multiplier is a much less influential factor. Thus, the dimensionless parameters involved in Lagrange multiplier can be chosen just for the sake of convenience of computation.

- Inflow turbulence is necessary considering the precise definition of wind loads. However, the proposed preconditioners and results in the work here provide an effective tool for the application of a simultaneous solution to wind-membrane interaction, laying a solid foundation for the introduction of a turbulence model in future work.

Acknowledgements

The research described in this paper was financially supported by National Natural Science Foundation of China (Contract No. 51108345), opening foundation of State Key Laboratory for Disaster Reduction in Civil Engineering of China (Contract No. SLDRCE-MB-04), Opening research fund of Southeast University, Key laboratory of concrete and pre-stressed concrete structure of Ministry of Education, Foundation of Liaoning province education administration (Contract No. L2013134), which are gratefully acknowledged.

References

Badia, S., Quaini, A. and Quarteroni, A. (2008a), "Modular vs. non-modular preconditioners for fluid–structure systems with large added-mass effect", *Comput. Method. Appl. M.*, **197**(49-50), 4216-4232.

Badia, S., Quaini, A. and Quarteroni, A. (2008b), "Splitting methods based on algebraic factorization for fluid–structure interaction", *SIAM J. Sci. Comput.*, **30**(4), 1778-1805.

Barker, A.T. and Cai, X.C. (2009), "NKS for fully coupled fluid–structure interaction with application", *Lecture Notes in Computational Science & Engineering*, **70**, 275-282**.**

Barker, A.T. and Cai, X.C. (2010), "Scalable parallel methods for monolithic coupling in fluid–structure interaction with application to blood flow modeling", *J. Comput. Phys.*, **229**(3), 642-659.

Borna, A., Habashi, W.G., McClure, G. and Nadarajah, S.K. (2013), "CFD-FSI simulation of vortex-induced vibrations of a circular cylinder with low mass-damping", *Wind Struct.*, **16**(5), 411-431.

Dagnew, A.K. and Bitsuamlak, G.T. (2013), "Computational evaluation of wind loads on buildings: a review", *Wind Struct.*, **16**(6), 629-660.

Dagnew, A.K. and Bitsuamlak, G.T. (2014), "Computational evaluation of wind loads on a standard tall building using LES", *Wind Struct.*, **18**(5), 567-598.

Degroote, J., Bathe, K.J. and Vierendeels, J. (2009), "Performance of a new partitioned procedure versus a monolithic procedure in fluid–structure interaction", *Comput. Struct.*, **87**(11-12), 793-801.

Farhat, C. and Vinod, K.L. (2014), "An ALE formulation of embedded boundary methods for tracking boundary layers in turbulent fluid–structure interaction problems", *J. Comput. Phys.*, **263**(15), 53-70.

Förster, C., Wall, W.A. and Ramm, E. (2005), "On the geometric conservation law in transient flow calculations on deforming domains", *Int. J. Numer. Meth. Fl.*, **50**(12), 1369-1379.

Geuzaine, C. and Remacle, J.F. (2009), "Gmsh: a three-dimensional finite element mesh generator with built-in pre- and post-processing facilities", *Int. J. Numer. Meth. Eng.*, **79**(11), 1309-1331.3366077

Habchi, C., Russeil, S. and Bougeard, D. (2013), "Partitioned solver for strongly coupled fluid–structure interaction", *Comput. Fluids*, **71**(30), 306-319.

Hachem, E., Feghali, S., Codina, R. and Coupez, T. (2013), "Anisotropic adaptive meshing and monolithic Variational Multiscale method for fluid–structure interaction", *Comput. Struct.*, **122**, 88-100.

Heil, M., Andrew, L.H. and Jonathan, B. (2008), "Solvers for large-displacement fluid–structure interaction

problems: segregated versus monolithic approaches", *Comput Mech.*, **43**(1), 91-101.
Hermann, G.M. and Jan, S. (2002), "Partitioned but strongly coupled iteration schemes for nonlinear fluid–structure Interaction", *Comput. Struct.*, **80**(27-30), 1991-1999.
Hermann, G.M. and Jan, S. (2003), "Partitioned strong coupling algorithms for fluid–structure interaction", *Comput. Struct.*, **81**(8-11), 805-812.
Lazarov, B.S. and Sigmund, O. (2011), "Factorized parallel preconditioner for the saddle point problem", *Int. J. Numer. Meth. Biomed. Eng.*, **27**(9), 1398-1410.
Manguoglu, M., Takizawa, K., Ahmed, H.S. and Tezduyar, T.E. (2011), "Nested and parallel sparse algorithms for arterial fluid mechanics computations with boundary layer mesh refinement", *Int. J. Numer. Meth. Fl.*, **65**(1-3), 135-149.
Michler, C., Hulshoff, S.J., Van, E.H. and Borst, R.de. (2004), "A monolithic approach to fluid-structure interaction", *Comput. Fluids*, **33**, 839-848.
Namkooong, K., Choi, H. and Yoo, J.Y. (2005), "Computation of dynamic fluid-structure interaction in two-dimensional laminar flows using combined formulation", *J. Fluid. Struct.*, **20**(1), 51-69.
Rees, T. and Greif, C. (2007), "A preconditioner for linear systems arising from interior point optimization methods", *SIAM J. Sci. Comput.*, **29**(5), 1992-2007.
Saad Y. (2003), "Iterative methods for sparse linear systems", Society for Industrial and Applied Mathematics, Minneapolis, Minnesota, U.S.
Sun, F.J. and Gu, M. (2014), "A numerical solution to fluid-structure interaction of membrane structures under wind action", *Wind Struct.*, **19**(1), 35-58.

JH